Radiology

Method for Tracking Eye Gaze during Interpretation of Endoluminal 3D CT Colonography: Technical Description and Proposed Metrics for Analysis[1]

Peter Phillips, PhD
Darren Boone, FRCS, FRCR
Susan Mallett, DPhil
Stuart A. Taylor, MB BS, MD, MRCP, FRCR
Douglas G. Altman, DSc
David Manning, PhD
Alastair Gale, PhD
Steve Halligan, MB BS, MD, FRCP, FRCR

Purpose: To develop an eye-tracking method applicable to three-dimensional (3D) images, where the abnormality is both moving and changing in size.

Materials and Methods: Research ethics committee approval was granted to record eye-tracking data from six inexperienced readers who inspected eight short (<30 seconds) endoluminal fly-through videos extracted from computed tomographic (CT) colonography examinations. Cases included true-positive and false-positive polyp detections from a previous study (polyp diameters, 5–25 mm). Eye tracking was performed with a desk-mounted tracker, and readers indicated when they saw a polyp with a mouse click. The polyp location on each video frame was quantified subsequently by using a circular mask. Gaze data related to each video frame were calculated relative to the visible polyp boundary and used to identify eye movements that pursue a polyp target as it changes size and position during fly-through. Gaze data were then related to positive polyp detections by readers.

Results: Tracking eye gaze on moving 3D images was technically feasible. Gaze was successfully classified by using pursuit analysis, and pursuit-based gaze metrics were able to help discriminate different reader search behaviors and methods of allocating visual attention during polyp identification. Of a total of 16 perceptual errors, 15 were recognition errors. There was only one visual search error. The largest polyp (25 mm) was seen but not recognized by five of six readers.

Conclusion: Tracking a reader's gaze during endoluminal interpretation of 3D data sets is technically feasible and can be described with pursuit-based metrics. Perceptual errors can be classified into visual search errors and recognition errors. Recognition errors are more frequent in inexperienced readers.

Supplemental material: *http://radiology.rsna.org/lookup/suppl/doi:10.1148/radiol.12120062/-/DC1*

[1] From the Health and Medical Sciences Group, University of Cumbria, Bowerham Rd, Lancaster LA1 3DJ, England (P.P.); Centre for Medical Imaging, University College London, London, England (D.B., S.A.T., S.H.); Department of Primary Care Health Sciences (S.M.) and Centre for Statistics in Medicine (D.G.A.), University of Oxford, Oxford, England; School of Medicine, Lancaster University, Lancaster, England (D.M.); and Applied Vision Research Centre, Loughborough University, Loughborough, England (A.G.).
Received February 2, 2012; revision requested March 23; revision received October 21; final version accepted October 30. Supported by a UK National Institute for Health Research (NIHR) Programme Grant for Applied Research (grant RP-PG-0407-10338). **Address correspondence to** P.P. (e-mail: *peter.phillips@cumbria.ac.uk*).

This article presents independent research commissioned by the National Institute for Health Research (NIHR) under its Programme Grants for Applied Research funding scheme (grant RP-PG-0407-10338). The views expressed are those of the authors and not necessarily those of the National Health Service, the NIHR, or the Department of Health. A proportion of this work was undertaken at University College London and University College London Hospital, which receive a proportion of funding from the NIHR Biomedical Research Centre funding scheme.

Eye tracking has been used to measure visual search patterns adopted by radiologists in a range of medical imaging situations, for example when searching for lung nodules on plain radiographs (1), breast lesions on mammograms (2), or fractures on radiographs (3). Eye tracking can help quantify differences in observer strategies related to expertise and help differentiate errors of search from those of recognition because it is known whether the observer looked directly at a lesion. Thus, eye tracking may have a role in training. For example, a study of 33 skeletal radiographs found that the most experienced observers had more true-positive detections despite having shorter dwell times (4). Traditionally, assessment of visual search has been applied to conventional two-dimensional images. However, the visual task faced by radiologists has undergone a paradigm shift during the past decade. In particular, data acquired with computed tomographic (CT) and magnetic resonance imaging platforms are inherently volumetric and increasingly displayed in three dimensions. Furthermore, interaction with the display is necessary to navigate the data. Such changes in visualization increase the perceptual and cognitive burden for the reader.

A vivid example is CT colonography, whereby the observer navigates through an endoluminal reconstruction of the colon. The navigation action results in a radial optical flow of visual information (5); new information appears from the focus of expansion as older but closer information exits the scene at the edges. The resulting motion of visual information requires a rotational eye movement (6) to stabilize a target on the fovea. The smooth pursuit movement does not occur during the inspection of two-dimensional images.

CT colonography is known to be difficult to interpret and requires considerable training (7), but little is known about the search strategies used by experienced and inexperienced readers.

In our research, we would like to separate perceptual error in CT colonography into either failure of search (ie, failure to "look" at a lesion) or failure of recognition (ie, failure to diagnose the lesion despite having looked at it). Thus, we performed this study to develop an eye-tracking method applicable to three-dimensional (3D) images, where the abnormality is both moving and changing in size.

Advances in Knowledge

- We describe a technique for analyzing gaze during interpretation of moving three-dimensional (3D) data sets, specifically CT colonography.
- We have developed metrics that describe pursuit (eye movement around a target that may change in size and position); in particular, we describe relative eye gaze by using a single distance measurement.
- Metrics that describe the characteristics of pursuits during polyp identification reveal that allocation of overt attention varies among readers.
- False-negative perceptual error in endoluminal interpretation can be described as either a visual search error or a recognition error by using gaze pursuits.

Materials and Methods

This article presents independent research commissioned by the National Institute for Health Research under its Programme Grants for Applied Research funding scheme (grant RP-PG-0407-10338). The views expressed are those of the authors and not necessarily those of the National Health Service, the National Institute for Health Research, or the Department of Health. A proportion of this work was undertaken at University College London and University College London Hospital, who receive a proportion of funding from the National Institute for Health Research Biomedical Research Centre funding scheme.

Institutional review board approval was granted to use anonymized CT colonography data, which had been collected during two previous studies (8,9), for eye tracking and to record data from six readers who were recruited from attendees at the 12th U.K. Virtual Colonoscopy Workshop, which was held November 16 and 17, 2009, in London, England. All readers were staff or resident radiologists, and all provided written informed consent. None had previously attended a CT colonography course, although the majority had interpreted 10–50 studies (range, 0–200 studies).

Case Preparation

To select cases that were neither too easy nor too difficult to interpret, our statistician (S.M.) selected 20 CT colonography cases in which a false-negative or false-positive polyp diagnosis had been made by approximately 50% of readers in the previous studies (8,9). Patients included both symptomatic and asymptomatic screening patients from four centers. All subjects had undergone CT colonography according to best practice guidelines (10,11). Each had endoscopic correlation, and the images from CT colonography were interpreted independently by three experienced readers to establish a reference standard diagnosis for each individual case.

A radiologist (D.B., with experience in >500 endoscopically validated cases) reviewed multiplanar reformations by using a medical image workstation (V3D

Published online before print
10.1148/radiol.12120062 **Content codes:** IN QA

Radiology 2013; 267:924–931

Abbreviations:
ROI = region of interest
3D = three-dimensional

Author contributions:
Guarantors of integrity of entire study, P.P., S.H.; study concepts/study design or data acquisition or data analysis/interpretation, all authors; manuscript drafting or manuscript revision for important intellectual content, all authors; manuscript final version approval, all authors; literature research, P.P., D.B., A.G., S.H.; clinical studies, P.P., D.B., S.A.T.; statistical analysis, P.P., S.M., A.G.; and manuscript editing, P.P., D.B., S.M., S.A.T., D.M., A.G., S.H.

Conflicts of interest are listed at the end of this article.

Colon; Viatronix, Stony Brook, NY) and reference standard reports to locate each true-positive lesion. Previous reader reports were evaluated to identify false-positive detections. Eleven cases were excluded because the lesion could not be demonstrated on either endoluminal projection or because it was within 5 seconds navigation of the rectal ampulla or cecal pole. If the lesion was visible on both prone and supine reconstructions, the less-conspicuous view was selected. A further case was excluded because of concurrent true- and false-positive polyps. Ultimately, five true-positive cases (with diameters of 6, 8, 11, 12, and 25 mm according to the reference standard) and two false-positive cases (with diameters of 5 and 7 mm according to the study reader) were selected. One false-positive case was viewed twice by each reader (eight video clips in total).

Video captures of automated endoluminal navigation (including the lesion) were then recorded at 75% maximum speed and edited to ensure the lesion became visible between 5 and 25 seconds at a random time point generated by using software (Stata; StataCorp, College Station, Tex). At least 5 seconds of video was recorded following the lesion's disappearance. The mean clip duration was 27 seconds (range, 24–31 seconds). The total video clip duration, time of lesion appearance, and time of lesion disappearance were noted. Uncompressed video was captured at 15 frames per second at 384 × 384 pixels.

Case Reading

The eight video clips were shown on an LCD monitor (SyncMaster 723N; Samsung, Suwon, Korea; 1280 × 1024 resolution, one pixel = 0.264 mm) approximately 60 cm in front of the reader. Videos were displayed on a black background in the display center and measured 384 × 384 pixels (10.1 × 10.1 cm), with a visual angle of 9.6°.

Eye tracking was performed by a medical image perception scientist (P.P., with 7 years of experience) by using an eye-tracking system (Tobii ×50; Tobii Technology, Danderyd, Sweden) located under the screen and Studio capture software (Tobii Technology) hosted on a laptop. Eye-tracker accuracy was 0.5°, approximately 20 screen pixels at a 60-cm viewing distance. Tracker angle and orientation were entered as parameters in the tracking software. The tracker sampling rate was 50 Hz.

Readers viewed cases in a quiet environment free from disturbance. They were unaware of the study hypothesis and the prevalence of abnormality—they were merely told that some cases would include polyps. No chin rest or head restraint was used. Spectacles and contact lenses were worn as normal. A five-point calibration routine matched reader gaze to screen location. When viewing the videos, readers were asked to identify any potential polyps that they would scrutinize further if encountered in daily practice and to indicate this with a mouse click. Readers did not target the polyp with the mouse pointer and had no control over navigation or playback speed within the video. Readers were asked to hold the mouse before video playback in order to prevent them from looking away from the screen to locate the mouse. Following an example "warm-up" video (excluded from analysis), the test cases were shown in two blocks with a different random order for each reader. Recording of eye movements only took place during playback. Readers could not see their data being recorded. The total time to complete all cases was approximately 10 minutes.

Data Preparation and Analysis

A medical image perception scientist (P.P.) examined each video frame by frame. The size and position of both true- and false-positive polyps were manually outlined with a circular region of interest (ROI) by using the coordinate system of the video frame. ROIs were described by using the circle center and radius. Each video thus generated a sequence of circular ROIs, one per frame, that contained a polyp. A radiologist experienced in the interpretation of CT colonographic images (D.B.) checked the ROIs to ensure they encompassed each polyp. The area of polyp visible in each individual frame was then calculated as the intersection of frame and ROI.

Eye tracking from each reader-case pair was checked to confirm that gaze data were contained within the video area. This acted as a secondary check on the initial calibration and monitored any drift in reported eye position during recording (Fig 1a). The reader's gaze moved to keep the abnormality in the foveal field of view with use of both fixation and smooth pursuit eye movements (6). The rotation component of gaze, when tracking a moving abnormality, made grouping gaze points with use of existing fixation methods (12) (eg, in terms of averaged x,y points) problematic. We therefore grouped gaze points into what we termed "pursuits" based on the distance to the polyp ROI boundary. This reframed measurements in terms of the relationship between gaze and polyp rather than gaze within the video (Fig 1b, Movie E1 [online]) and could cover the transitions of size and speed that a polyp undergoes owing to navigation. For each point of gaze data acquired during a visible polyp, the distance from the gaze point to the closest ROI margin point was calculated. Short runs of missing gaze data due to head movement were reconstructed by using multiple imputation methods.

To identify gaze outside the polyp ROI, but where the polyp boundary fell within very high visual acuity, a 1.25° acceptance radius (13) equivalent to 50 pixels was added to the ROI radius. Points were marked as related to the polyp region if they were within this 50-pixel threshold. Contiguous region-related points, with a minimum number of four points (an 80-msec fixation threshold) were identified as pursuits. These were used to calculate *(a)* the time to first hit (time from first polyp appearance to when first seen by the reader), *(b)* the cumulative gaze dwell time on ROIs, and *(c)* the number of times the reader looked at the ROI. The time from first hit to mouse click (ie, decision time) was also calculated.

A positive detection was registered if gaze intersected an ROI threshold and a mouse click was registered. Two types of false-negative detections were identifiable: A perceptual error occurred

Figure 1

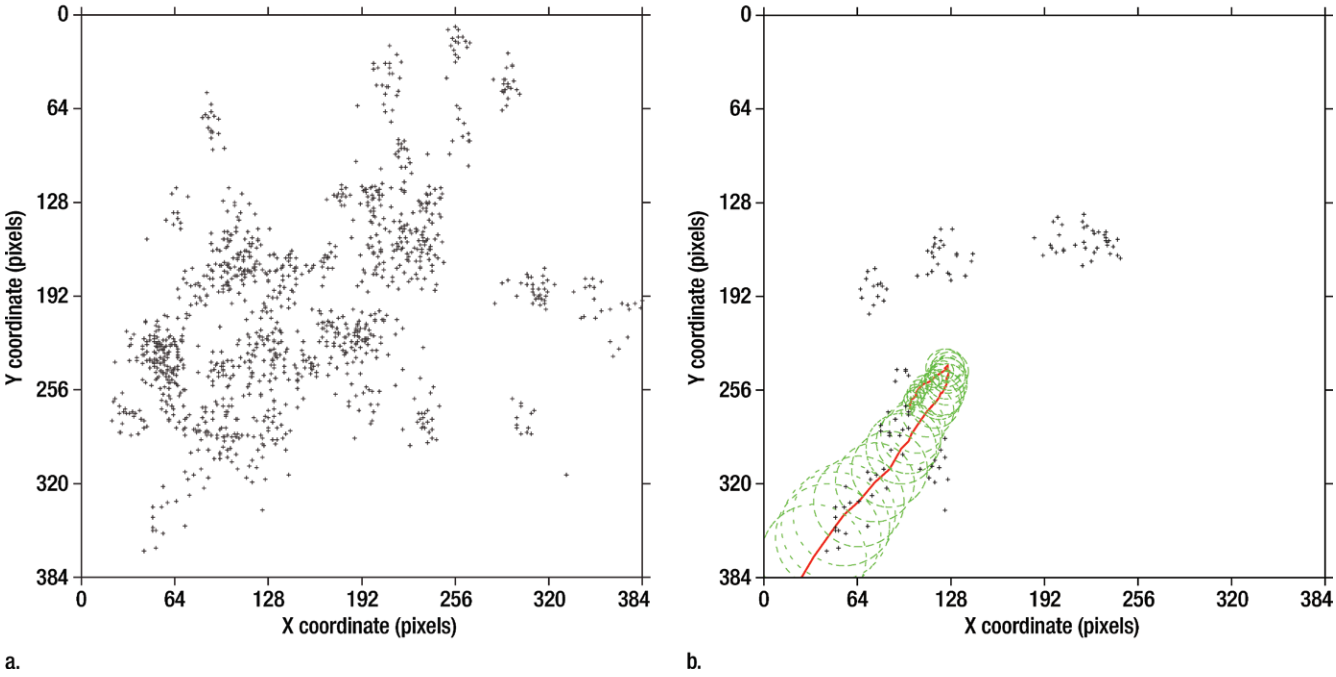

Figure 1: **(a)** Graph shows distribution of a reader's gaze in a 25-second video clip with a 12-mm polyp. Each dot represents a gaze point (sample rate, 50 Hz). **(b)** Graph shows frame-by-frame ROIs for 12-mm polyp and distribution of gaze when polyp is on screen. Each dot is ROI for each individual frame (frame rate, 15 Hz). Line indicates path of polyp center.

when no gaze intersected with the moving ROI, and a recognition error occurred when gaze data intersected an ROI but no mouse click was registered. All other mouse clicks were considered false-positive findings.

Statistical Analysis

Missing data were imputed by using multiple imputation methods (14) adapted for missing longitudinal data. Eye pursuits were defined when the gaze was within 50 pixels from the polyp ROI boundary for at least 80 msec. To allow for measurement error, the end of each pursuit was defined as at least 20 msec when the average pursuit distance plus 2 standard deviations was more than 50 pixels. Eye metrics were defined as in Figure 2; cumulative dwell was the total time within a 50-pixel distance from the polyp ROI boundary. The number of pursuits was averaged across five imputed data sets, rounded to an integer. Data were analyzed with software (Stata 11.0, StataCorp).

Figure 2

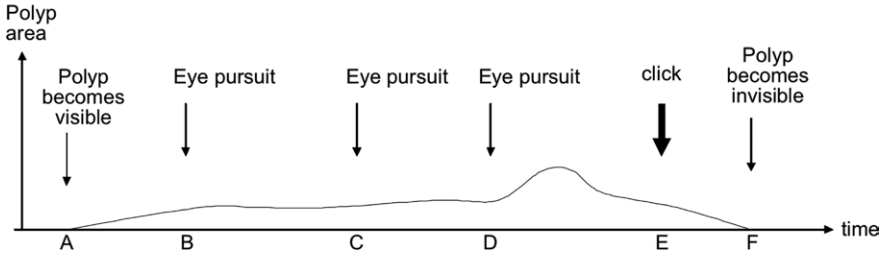

Figure 2: Schematic time course of identified gaze and mouse clicks recorded when polyp is visible on screen (time *A* to time *F*). In this case, the reader's gaze first "sees" the polyp at time *B*. Reader gaze revisits the polyp two more times (times *C* and *D*) between viewing other regions of the colon video. The reader clicks the mouse to indicate suspicion, occurring at time *E*. The polyp disappears from the field of view at time *F*. The time to first hit is time *B* minus time *A*. The overall reader decision time is time *E* minus time *B*. The reader gazed at the polyp three times (times *B*, *C*, and *D*).

Results

Before taking the CT colonography course, one of the six readers had interpreted fewer than 10 CT colonography cases, three readers had interpreted 11–50 cases, and two readers had interpreted 101–200 cases. Eye tracking was technically feasible, calibration was accurate, and data were acquired from all readers. Of the eight possible positive polyp identifications, the highest score (seven identifications) was obtained by a reader with experience in interpreting 11–50 cases; the lowest score (four identifications) was obtained by a

Table 2

Time to First Pursuit and Cumulative Dwell Time for Each Polyp and Each Reader

Parameter	Reader 1	Reader 2	Reader 3	Reader 4	Reader 5	Reader 6	Average	Percentage of Time Polyp Was Visible
Case 1								
Time to first pursuit	0.94	0.16*	0.10*	0.12*	0.50*	0*	0.3	12
Dwell time	0.08	1.76*	1.62*	1.00*	1.24*	2.07*	1.29	53
Case 2								
Time to first pursuit	1.00	0*	2.11*	0.76*	0*	0	0.65	19
Dwell time	1.80	2.08*	0.43*	1.97*	2.35*	1.48	1.69	50
Case 3								
Time to first pursuit	0.14	0.30	0.90	0.56*	0.56	0.60	0.51	12
Dwell time	2.35	2.30	1.57	2.39*	1.30	0.98	1.81	43
Case 4								
Time to first pursuit	1.68*	3.25*	1.54*	0.02*	1.89	0.40*	1.46	16
Dwell time	3.97*	2.16*	2.93*	0.78*	0.82	1.40*	2.01	23
Case 5								
Time to first pursuit	0.46*	0.24*	0.04*	1.14*	0*	0*	0.31	4
Dwell time	5.58*	5.34*	4.26*	5.36*	5.52*	3.53*	4.93	68
Case 6								
Time to first pursuit	0.40*	0.40*	0.51*	0.32*	0*	0.46*	0.35	4
Dwell time	4.13*	4.19*	2.17*	3.15*	3.01*	4.87*	3.62	46
Case 7								
Time to first pursuit	0.36*	2.57	0.50*	0.22*	0.02	0.46*	0.69	9
Dwell time	3.47*	1.78	2.35*	2.55*	3.21	4.91*	3.04	38
Case 8								
Time to first pursuit	1.66	1.32	1.56	2.21	0*	NA	1.35	15
Dwell time	0.52	0.38	0.34	0.44	0.88*	NA	0.43	5

Note.—Except where indicated, data are seconds. Cases 1–5 are true-positive cases, and cases 6–8 are false-positive cases. A time to first pursuit value of zero indicates that the polyp was seen as soon as it became visible on the screen. NA = not applicable, polyp was missed.

* Positive polyp identification.

Table 1

Summary of Search and Recognition Errors for Six Readers

	True-Positive Cases					False-Positive Cases		
Parameter	Case 1	Case 2	Case 3	Case 4	Case 5	Case 6	Case 7	Case 8
Polyp diameter (mm)	12	6	25	11	8	7	7	5
Length of time polyp was visible (sec)	2.47	3.40	4.20	8.87	7.27	7.93	7.93	2.93
No. of errors	1	2	5	1	0	0	2	5
Search errors	0	0	0	0	0	0	0	1
Recognition errors	1	2	5	1	0	0	2	4

reader with experience in interpreting 101–200 cases.

Perception and recognition errors for each polyp are shown in Table 1. Sixteen of the 48 decisions (33%) were errors, with the vast majority (15 decisions) being errors of recognition. A search error occurred in only one case. Interestingly, the smallest (5 mm) and largest (25 mm) polyps were the most error prone, which suggests that error is not related to diameter alone. The single perceptual (search) error occurred in the case with the smallest (5 mm) false-positive polyp.

Table 2 shows the time to first pursuit and cumulative gaze dwell time for each reader-case: Only one polyp was not pursued by a reader (reader 6 and false-positive case 8). Eight of the 48 pursuits (17%) commenced immediately when the polyp became visible on the screen, seven of which resulted in positive identification. The longest time elapsed before a polyp was looked at was 3.25 seconds. The shortest cumulative gaze dwell time was 0.08 second (ie, the shortest permitted; four contiguous points at 0.02 second each) but did not result in a positive identification. The shortest cumulative dwell with a positive identification was 0.43 second.

Table 3 shows the number of times a polyp was viewed during its time on screen. There was only one search error. The largest polyp (case 3) was viewed by all readers at least twice but was indicated by only one reader with a mouse click (Table 4). With the

exception of reader 4 looking at case 2, detection decisions indicated with a mouse click were associated with more than one gaze at the polyp.

Table 4 shows the decision time for each reader. The polyp on screen for the shortest time (case 1, 2.47 seconds) had the shortest average decision time of 2.0 seconds for readers who indicated this polyp (but a high average decision time of 81% when expressed as a percentage of polyp visibility). This case had the shortest average time to first pursuit time (0.3 second) and, on average, the cumulative eye dwell was 52% of the time the polyp was on the screen.

The polyp on screen for the longest time (case 4, 8.87 seconds) had decision times ranging from 2.10 to 7.86 seconds (Table 4). The reader of this case with the shortest decision time (reader 2) saw the polyp 3.25 seconds after it had appeared and gazed at the polyp 10 times for a total of 2.16 seconds. Reader 6 had the longest decision time for this polyp. This reader saw the polyp 0.40 second after it had appeared and used three gazes with a cumulative dwell time of 1.40 seconds (Tables 2, 3).

One video was viewed twice by all readers (polyps 6 and 7). Times to first pursuit and the number of gazes were similar within readers, although two of the six readers had decision errors in one viewing and not in the other (Table 4).

Plotting gaze on the video area (Fig 1a) does not show the temporal relationship between points. Although some clustering of points was apparent, the ordering is unknown. It was possible to visualize the temporal aspect of the data by plotting *x* and *y* coordinates as separate lines (Fig 3, top). Because time was preserved, the polyp center position and maximum extent could be plotted as separate *x* and *y* areas. Thus, polyps are plotted as areas rather than discrete lines or points, with each box being 66.7-msec wide—the interval of one video frame (Fig 3, top). The extent of the area added owing to the distance thresholding is also plotted.

The calculated distance from the polyp boundary to the gaze points is shown in Figure 3, bottom. Two pursuits could be identified. The first was the initial 200 msec when the polyp was on screen. The reader's gaze was already in the region where the polyp appeared and tracked the polyp approximately 40 pixels from the polyp boundary. The second pursuit was approximately from 16550 to 17200 msec, a duration of 650 msec. In this instance, the pursuit followed the edge of the polyp as it moved and increased in area.

Table 3

Number of Times Each Polyp Was Viewed by Each Reader during Its Time on Screen

	True-Positive Cases					False-Positive Cases		
Reader	Case 1	Case2	Case 3	Case 4	Case 5	Case 6	Case 7	Case 8
1	1	5	2	5*	2*	8*	7*	1
2	3*	7*	5	10*	7*	7*	8	2
3	4*	4*	3	9*	7*	7*	6*	2
4	2*	1*	4*	2*	4*	9*	5*	1
5	3*	2*	2	2	6*	9*	9	2*
6	3*	4	2	3*	7*	10*	5*	NA

Note.—A view was defined by the reader's gaze crossing the region threshold and remaining within it for a minimum of four points (80 msec). NA = not applicable, polyp was missed.

* Positive polyp identification.

Table 4

Decision Times for Each Reader and Polyp

	True-Positive Cases					False-Positive Cases		
Reader	Case 1	Case 2	Case 3	Case 4	Case 5	Case 6	Case 7	Case 8
1	RE	RE	RE	7.31	4.90	6.09	6.23	RE
2	1.84	3.13	RE	2.10	3.91	6.16	RE	RE
3	2.21	1.20	RE	4.73	5.47	6.67	5.73	RE
4	2.26	1.86	2.86	5.65	4.78	6.42	6.07	RE
5	1.74	2.35	RE	RE	6.36	6.94	RE	2.15
6	1.97	RE	RE	7.86	6.01	7.27	6.03	SE
Average decision time	2.00	2.14	2.86	5.53	5.24	6.59	6.01	2.15
Percentage of time polyp was visible	81	63	68	62	72	83	76	73

Note.—Except where indicated, data are seconds. RE = recognition error, SE = search error.

Discussion

To investigate the interpretation of modern 3D medical image displays, we have developed a method for analyzing visual gaze when the abnormality is both moving and changing in size. Our method allows for multiple fixation and smooth pursuit eye movements during abnormality inspection. We have shown that data collection is feasible and have developed metrics derived from plotting gaze and calculating intersections with the region of abnormality.

Polyps were described frame by frame with use of circular ROIs, and individual gaze points were grouped into "pursuits" on the basis of the distance to the time-appropriate ROI boundary. It is the boundary, the edge of the polyp against the background, that contains useful visual information. While pursuing a polyp, the reader was focused on the polyp edge rather than the center even though the polyp changed in size and position over the lifetime of the pursuit. Metrics such as time to first hit and number of dwells, which are used

Figure 3

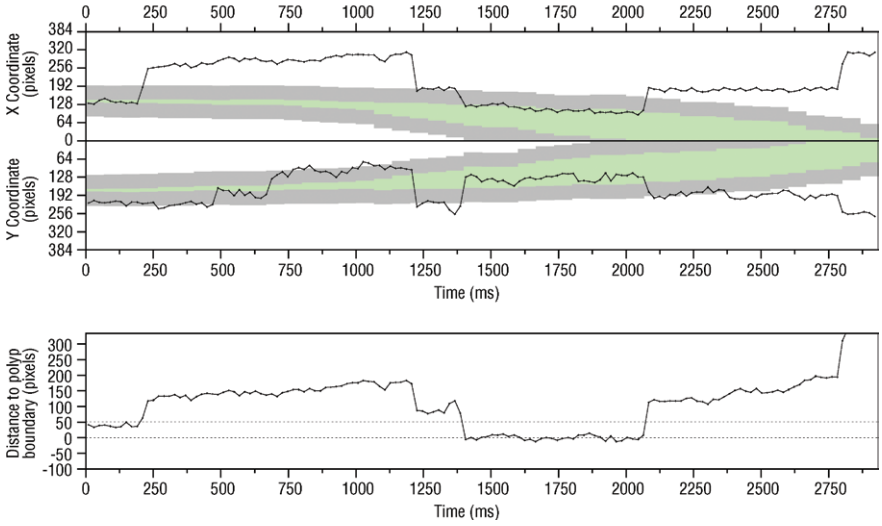

Figure 3: Top: Time course of reader eye gaze and polyp extent for reader 5 and case 8 (5-mm polyp). Lines represent reader gaze position in *x* (top) and *y* (bottom) video coordinates. The maximum extent of the polyp in horizontal *(x)* and vertical *(y)* directions for each video frame is shown in green and is bounded by the 50-pixel distance threshold (gray border). The *x* and *y* extent increases as polyp approaches edges of screen. Both *x* and *y* gaze components must be contained within the polyp plus threshold region for a minimum of four points to be deemed a pursuit. Bottom: Calculated distance from gaze to polyp boundary (solid line) over same time axis as top image. Upper dashed line is 50-pixel distance threshold, lower dashed line represents boundary of polyp. A point with a negative distance value indicates that the point is within the polyp region.

in pulmonary nodule (15) and mammographic (16) interpretation, have been reinterpreted for gaze pursuits of moving lesions with changing size.

The endoluminal visualization is a reconstruction of the view from a colonoscope. Eye tracking has been used to investigate the distribution of visual attention while viewing offline videos of colonoscopy withdrawal (17). High-performing readers were shown to allocate most of their attention to the central third of the video screen, but experienced readers spent a lower percentage of time in that area. Our method measures attention to the target abnormality as it moves within an endoluminal video. Colonoscopic inspection is performed during withdrawal of the scope, reversing the direction of optical flow. The flow of information in the endoluminal view has similarities to human motion through a natural scene, such as walking (18) or driving (19). The target abnormality is part of the colon wall. It moves with the scene owing to viewpoint motion, like a sign on the roadside when driving. Fletcher and Zelinsky (20) used a similar gaze-to-target distance method to establish whether a driver had seen a road sign.

The natural environment can provide context for visual search tasks. A horizon helps orient the observer and can inform their search for targets (cars are more likely to be on the ground than the sky). The changing landscape of a natural scene provides context that influences search (eg, a stop sign is more likely to occur at a road intersection). Placing a stop sign by the roadside out of context reduces the likelihood of a driver seeing it (19). Contextual information in the endoluminal view comes from the shape and texture of the visible bowel wall. A polyp may occur in any part of the colon and in any area of the visualization.

Endoluminal navigation requires a search strategy that samples ROIs before they move out of view. However, competition from other features, perhaps those closer to the edge and therefore larger and more detailed, may mean that ROIs must be revisited later. Readers must judge the optimal time to look at a feature, trading size and detail against remaining screen time.

Competition for attention can also come from nontargets looming in the field of view. Looming objects, which increase in size with little positional change, imply a risk of collision with the observer in the future. Observers have been shown to adapt their gaze strategy on the basis of the behavior of frequently encountered targets in tasks with a real risk of collision (18). Looming objects in a no-risk, abstract scene still demand attention. Lin et al (21) simulated looming in an abstract scene presented on a computer monitor. Observer attention was attracted to looming objects, particularly those that approached from the periphery, where the trajectory implied a future collision. Gaze was also directed to objects looming from the bottom of the screen, at the 6 o'clock position. Such trajectories implied a collision with the observer's body, despite there being no real-world risk. The endoluminal visualization can produce looming features: a projection into the lumen owing to poor colon preparation, a constriction of the lumen owing to a fold, or when approaching an area of collapsed wall. Navigation around a tight corner can also (re)introduce visual information from the periphery of the video.

Gaze tracking demonstrates how readers allocate attention. Our metrics resolved differences in reader visual search behavior. The example of two readers (readers 2 and 6) of the longest case on screen (case 4) shows different approaches to identification. There is marked difference in the number of pursuits, but both result in a positive identification. Reader 2 made his decision quickly and early, but with multiple gazes (10 gazes; average dwell time, 216 msec), indicating that he attended to other features during his decision. Reader 6 saw the polyp early but attended to other areas for longer, making fewer (but longer) gazes at the polyp (three gazes; average dwell time, 467 msec) and not making a decision until the

polyp was about to go off screen. Both readers had similar experience (11–50 cases) and identifications (five of eight correct identifications).

This study does have limitations. We investigated endoluminal fly-through, but only in automatic mode and with use of a small number of cases. Readers indicated a potential abnormality but could not adjust the speed or stop and inspect as per usual daily practice. In addition, irregular polyps and those seen in profile were difficult to characterize by using a single circular ROI. Other boundary descriptions are possible to improve boundary accuracy but will require more complex calculations. The 50-pixel distance threshold was constant across all polyp sizes. A side effect of this decision is that distant polyps can be called as "seen" too early. Possible perceptual errors would be classified as recognition errors. A threshold based on a percentage of the polyp region radius would have the opposite effect: Larger polyps would have a large threshold. Any future thresholding technique must be able to account for polyps at both small and large scales. We limited our investigation to inexperienced readers; it will be informative to investigate differences among experienced readers.

In summary, eye-tracking volumetric data present challenges for recording what is on the screen where and when and for synchronizing that data with gaze data. The properties of volume modalities, particularly that not all imaging data are visible simultaneously, challenge established metrics. We have reframed the problem by considering the relationship between gaze and lesion rather than screen and/or image area. The metrics we developed can describe differences in reader gaze behavior and attention distribution when interpreting an automatic CT colonography fly-through. Perceptual errors can be classified into visual search errors and recognition errors. Recognition errors are most frequent in inexperienced readers.

Disclosures of Conflicts of Interest: P.P. No relevant conflicts of interest to disclose. **D.B.** No relevant conflicts of interest to disclose. **S.M.** No relevant conflicts of interest to disclose. **S.A.T.** Financial activities related to the present article: none to disclose. Financial activities not related to the present article: is a paid consultant for Medicsight. Other relationships: none to disclose. **D.G.A.** No relevant conflicts of interest to disclose. **D.M.** No relevant conflicts of interest to disclose. **A.G.** No relevant conflicts of interest to disclose. **S.H.** Financial activities related to the present article: none to disclose. Financial activities not related to the present article: is a paid consultant for Medicsight; received payment for expert testimony from various firms. Other relationships: none to disclose.

References

1. Kundel HL, Nodine CF, Krupinski EA. Searching for lung nodules: visual dwell indicates locations of false-positive and false-negative decisions. Invest Radiol 1989;24(6):472–478.
2. Krupinski EA. Visual scanning patterns of radiologists searching mammograms. Acad Radiol 1996;3(2):137–144.
3. Hu CH, Kundel HL, Nodine CF, Krupinski EA, Toto LC. Searching for bone fractures: a comparison with pulmonary nodule search. Acad Radiol 1994;1(1):25–32.
4. Leong JJH, Nicolaou M, Emery RJ, Darzi AW, Yang GZ. Visual search behaviour in skeletal radiographs: a cross-specialty study. Clin Radiol 2007;62(11):1069–1077.
5. Warren WH Jr, Hannon DJ. Eye movements and optical flow. J Opt Soc Am A 1990;7(1):160–169.
6. Palmer SE. Vision science: photons to phenomenology. Cambridge, Mass: MIT Press, 1999.
7. European Society of Gastrointestinal and Abdominal Radiology CT Colonography Group Investigators. Effect of directed training on reader performance for CT colonography: multicenter study. Radiology 2007;242(1):152–161.
8. Halligan S, Altman DG, Mallett S, et al. Computed tomographic colonography: assessment of radiologist performance with and without computer-aided detection. Gastroenterology 2006;131(6):1690–1699.
9. Halligan S, Mallett S, Altman DG, et al. Incremental benefit of computer-aided detection when used as a second and concurrent reader of CT colonographic data: multiobserver study. Radiology 2011;258(2):469–476.
10. Barish MA, Soto JA, Ferrucci JT. Consensus on current clinical practice of virtual colonoscopy. AJR Am J Roentgenol 2005;184(3):786–792.
11. Taylor SA, Laghi A, Lefere P, Halligan S, Stoker J. European Society of Gastrointestinal and Abdominal Radiology (ESGAR): consensus statement on CT colonography. Eur Radiol 2007;17(2):575–579.
12. Salvucci DD, Goldberg JH. Identifying fixations and saccades in eye-tracking protocols. In: Proceedings of the Eye Tracking Research and Applications Symposium. New York, NY: Association for Computing Machinery, 2000; 71–78.
13. Chakraborty D, Yoon H-J, Mello-Thoms C. Spatial localization accuracy of radiologists in free-response studies: inferring perceptual FROC curves from mark-rating data. Acad Radiol 2007;14(1):4–18.
14. White IR, Royston P, Wood AM. Multiple imputation using chained equations: issues and guidance for practice. Stat Med 2011;30(4):377–399.
15. Krupinski EA, Berger WG, Dallas WJ, Roehrig H. Searching for nodules: what features attract attention and influence detection? Acad Radiol 2003;10(8):861–868.
16. Krupinski EA. Visual search of mammographic images: influence of lesion subtlety. Acad Radiol 2005;12(8):965–969.
17. Almansa C, Shahid MW, Heckman MG, Preissler S, Wallace MB. Association between visual gaze patterns and adenoma detection rate during colonoscopy: a preliminary investigation. Am J Gastroenterol 2011;106(6):1070–1074.
18. Jovancevic-Misic J, Hayhoe M. Adaptive gaze control in natural environments. J Neurosci 2009;29(19):6234–6238.
19. Shinoda H, Hayhoe MM, Shrivastava A. What controls attention in natural environments? Vision Res 2001;41(25-26):3535–3545.
20. Fletcher L, Zelinsky A. Driver inattention detection based on eye gaze-road event correlation. Int J Robot Res 2009;28(6):774–801.
21. Lin JY, Franconeri S, Enns JT. Objects on a collision path with the observer demand attention. Psychol Sci 2008;19(7):686–692.